Bootstrap current for neoclassically optimized stellarator systems*

M. Drevlak[1], M. F. Heyn[2], S. V. Kasilov[3], **W. Kernbichler**[2], D. Monticello[4], V. V. Nemov[3], C. Nührenberg[1], J. Nührenberg[1], A. Reiman[4]

[1]Max-Planck-Institut für Plasmaphysik, Association EURATOM-IPP
Greifswald, GERMANY
[2]Institut für Theoretische Physik, Technische Universität Graz
Association EURATOM-ÖAW, Graz, AUSTRIA
[3]Institute of Plasma Physics, NSC "Kharkov Institute of Physics and Technology",
Kharkov, UKRAINE
[4] Princeton Plasma Physics Laboratory, Princeton NJ, USA

Introduction

Minimization of neoclassical transport in the $1/\nu$ regime (effective ripple minimization) is one of the key issues in stellarator optimization. Another important task in some optimization procedures is the minimization of bootstrap current, because bootstrap current may lead to an aggravation of plasma control and to worsening of stability properties. In the present report, a comparative study of the bootstrap current is carried out for two optimized stellarator schemes, namely for the W7-X configuration (see, e.g., [1]) and for the quasi-helically symmetric stellarator (QHS) [2]. The W7-X configuration has a somewhat larger effective ripple, however, it is additionally optimized with respect to bootstrap current. Here, computations are done for different magnetic configurations including a vacuum magnetic field and magnetic fields resulting from finite beta equilibria. For those configurations, the geometrical factor for the bootstrap current is determined by integration along magnetic field lines [3,4]. The equilibria forming the basis of the bootstrap evaluation do not take a bootstrap current into consideration so that in this sense the result is only consistent for vanishing bootstrap current.

Basic formulas

In the $1/\nu$ regime, a formula for bootstrap current can be presented in the following form

$$\left\langle \frac{j_b}{B} \right\rangle = -c\lambda_b \frac{1}{B_0^2}\left[\alpha_n (T_e+T_i)\frac{dn}{dr} + \alpha_T^e n \frac{dT_e}{dr} + \alpha_T^i n \frac{dT_i}{dr}\right], \qquad (1)$$

where j_b is the bootstrap current density, λ_b is a dimensionless geometric factor, B_0 is a reference magnetic field, c is speed of light, α_n, α_T^e and α_T^i are dimensionless factors. These dimensionless α-factors are of order of unity when the fraction of trapped particles, f_t, is small and the fraction of circulating particles, f_c, is close to unity. In cases with an increased trapped particle fraction, the α-factors are proportional to $1/f_c$.

For specific stellarator devices, a computation of the geometrical factor λ_b is very important for an analysis of the influence of the magnetic field geometry on the bootstrap

*This work was partly supported by the project INTAS-99-00592, by the Austrian Academy of Sciences and by the Association EURATOM-ÖAW. The content of the publication is the sole responsibility of its publishers and it does not necessarily represent the views of the Commission or its services.

current. On a given magnetic surface, the dimensionless quantity λ_b is determined by integration along the magnetic field line length, s. The definition of λ_b is as follows

$$\lambda_b = \frac{\langle \lambda_{PS} B^2 \rangle}{\langle B^2 \rangle} + \lambda_B \ , \tag{2}$$

with

$$\langle A \rangle = \lim_{L\to\infty} \left(\int_0^L \frac{\mathrm{d}s}{B} \right)^{-1} \int_0^L \mathrm{d}s \frac{A}{B} \ , \tag{3}$$

$$\lambda_{PS}(s) = \frac{2B_0^2}{\langle |\nabla\psi| \rangle} Y_{PS}(s) \ , \qquad Y_{PS}(s) = \int_{s_m}^{s} \mathrm{d}s' \frac{|\nabla\psi| k_G}{B^2} \ , \tag{4}$$

$$\lambda_B = \frac{3B_0^2}{8\langle |\nabla\psi| \rangle} \lim_{L\to\infty} \frac{1}{v^3} \int_0^{J_{\perp min}^{abs}} \mathrm{d}J_\perp J_\perp^2 \frac{1}{I_L} \int_{s_m}^{L} \mathrm{d}s \frac{|v_\parallel|}{B} Y_B(s) \ , \tag{5}$$

$$Y_B(s) = \int_{s_m}^{s} \mathrm{d}s' \frac{B|\nabla\psi| k_G}{|v_\parallel|^3} \ , \qquad I_L = \int_{s_m}^{L} \mathrm{d}s \frac{|v_\parallel|}{B} \ . \tag{6}$$

Here, ψ is the magnetic surface label, $k_G = (\mathbf{h} \times (\mathbf{h} \cdot \nabla)\mathbf{h}) \cdot \nabla\psi / |\nabla\psi|$ is the geodesic curvature of a magnetic field line with the unit vector $\mathbf{h} = \mathbf{B}/B$, $v_\parallel^2 = v^2 - J_\perp B$, $J_\perp = v_\perp^2/B$, $J_{\perp min}^{abs} = v^2/B_{max}^{abs}$ corresponds to the trapped-passing boundary, B_{max}^{abs} is the global maximum of B on the particular magnetic field line, and s_m is the position of this maximum. Expressions (2) - (6) were obtained in Refs. [3,4] and are intended for computations for magnetic fields given in real-space coordinates. One advantage of these expressions is the following. Whenever magnetic fields are available in real-space coordinates, calculations can be performed without a field transformation to magnetic coordinates. However, after transformation to Hamada or Boozer magnetic coordinates, one can also do computations for equilibria in magnetic coordinates. For these cases, one can show the relationship between λ_b and the corresponding factors in Refs. [5-8].

Basic parameters

For the analysis of W7-X, three different cases of the W7-X standard high-mirror configuration are used: (i) a vacuum magnetic field directly produced by modular coils of the device, (ii) a magnetic field produced by the PIES code [9] for a free boundary equilibrium with $< \beta >$=1%, and (iii) a magnetic field in Boozer magnetic coordinates for a finite $< \beta >= 4.8\%$ equilibrium with a fixed boundary [10]. The quasi-helically symmetric device QHS is analyzed using a magnetic field representation in Boozer coordinates for a fixed boundary equilibrium with $< \beta >$=0.058 [2].

Computational results

All computations of λ_b are carried out on non-resonant magnetic surfaces. Results for λ_b are presented in Figures 1 and 2 as functions of the ratio r/a where r is the mean radius of a given magnetic surface and a is the mean radius of the pertinent outermost magnetic surface. In both Figures, the result for the equilibrium in Boozer coordinates is presented as curve 2. These results are very close to the analogous curves in Refs. [3,11] for a W7-X vacuum magnetic field represented in terms of toroidal harmonic functions. From the analysis in Refs. [3,11] follows that in the whole confinement region the ratio of λ_b for W7-X to λ_b for an equivalent tokamak does not exceed 0.25. It should be noted that this is in accordance with the results of Ref.[1], where the bootstrap current for W7-X was investigated with a global Monte Carlo simulation as well as with the DKES code.

When comparing absolute values of λ_b for W7-X, one can clearly see from Figures 1 and 2 that direct results for modular coils as well as results for a free boundary PIES equilibrium are smaller than results for the fixed-boundary case in Boozer coordinates. However, rather big irregularities of λ_b are seen in the vicinity of resonant magnetic surfaces with a rotational transform close to rational numbers. These irregularities are more pronounced for the PIES data at ι close to 15/17 ($r/a \approx$0.35), 10/11 ($r/a \approx$0.75), 25/27 ($r/a \approx$0.84) and 15/16 ($r/a \approx$0.9). For the vacuum field, this is seen for ι close to 25/27 ($r/a \approx$0.87) and 20/21 ($r/a \approx$0.94). The observed irregularities are directly connected with bootstrap current resonances which can arise at resonant magnetic surfaces in the limit of low particle collision frequencies [11].

Results for the $<\beta>$=0.058 equilibrium of QHS are shown in Figure 3 (curve 1) as function of $\sqrt{s}$ where s is the normalized toroidal magnetic flux ($s^{1/2} \approx r/a$). A rather big irregularity of λ_b for $s^{1/2}$ from 0.7 to 0.8 can be explained by the fact that the corresponding flux surfaces are in the vicinity of a rational surface with ι=18/14. For comparison, curve 2 in Figure 3 shows results for λ_b from Ref. [11] for the vacuum magnetic field of QHS [2]. In addition, curve 3 shows results for the finite beta W7-X equilibrium with a fixed boundary (curve 2 in Figure 1 as well as 2). It can be clearly seen that absolute values of λ_b for QHS are significantly larger than for W7-X. However, with increasing β this difference somewhat decreases.

Note that for all configurations in this report, the rotational transform ι has an anti-clockwise direction (with increasing toroidal angle). Therefore, for a negative (positive) λ_b the sign of the bootstrap current is such that it increases (decreases) the rotational transform.

Summary

A clear advantage of the field line integration method for computing the geometrical factor λ_b for bootstrap current in the $1/\nu$ regime is the possibility to use data for magnetic configurations in various forms. This can be either coil data for use in a Biot-Savart code, a vacuum magnetic field represented in terms of toroidal harmonic functions, or zero or finite β equilibria from VMEC (Boozer coordinates) as well as PIES. This technique therefore delivers a unique tool for a comparative study. Here, such a study is performed for W7-X, clearly showing the reduction of bootstrap current in such an optimized device. In addition, one can study the influence of different equilibria on the results and the possible appearance of bootstrap resonances in the low collisionality regime.

References

[1] H. Maassberg, W. Lotz, and J. Nührenberg, Phys. Fluids B **5**, 3728 (1993).

[2] J. Nührenberg and R. Zille, Phys. Lett. A **129**, 113 (1988).

[3] S. V. Kasilov, V. V. Nemov, W. Kernbichler, M. F. Heyn, in 27th EPS Conference on Controlled Fusion and Plasma Physics (Editors: K.Szegö, T.N.Todd and S.Zoletnik), Budapest, Hungary, 12-16 June 2000, ECA **24B**, 668 (2000).

[4] W. Kernbichler, V. V. Nemov, S. V. Kasilov, M. F. Heyn, Problems of Atomic Science and Technology. Series: Plasma Physics (6),8 (2000).

[5] K. C. Shaing and J. D. Callen, Phys. Fluids **26**, 3315 (1983).

[6] A. H. Boozer and H. J. Gardner, Phys. Fluids B **2**, 2408 (1990).

[7] N. Nakajima and M. Okamoto, J. Phys. Soc. Jpn. **61**, 833 (1992).

[8] J. L. Johnson, K. Ichiguchi, Y. Nakamura, M. Okamoto, M. Wakatani, and N. Nakajima, Phys. Plasmas **6**, 2513 (1999).

[9] A. H. Reiman and H. S. Greenside, J. Comput. Phys. **75**, 423 (1988).

[10] V. V. Nemov, S. V. Kasilov, C. Nührenberg, J. Nührenberg, W. Kernbichler and M. F. Heyn, Plasma Phys. Control. Fusion **45**, 43 (2003).

[11] W. Kernbichler, S. V. Kasilov, V. V. Nemov, G. Leitold, M. F. Heyn, in 29th EPS Conference on Plasma Phys. and Contr. Fusion, Montreux, Switzerland, 17-21 June 2002, ECA **26B**, P2.100 (2002).

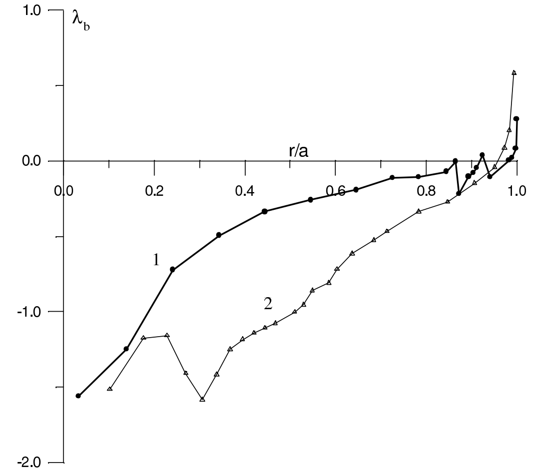

Fig. 1: Parameter λ_b for W7-X for the magnetic field produced by modular coils (curve 1) and for Boozer data corresponding to a finite β equilibrium with a fixed boundary (curve 2 marked by triangles).

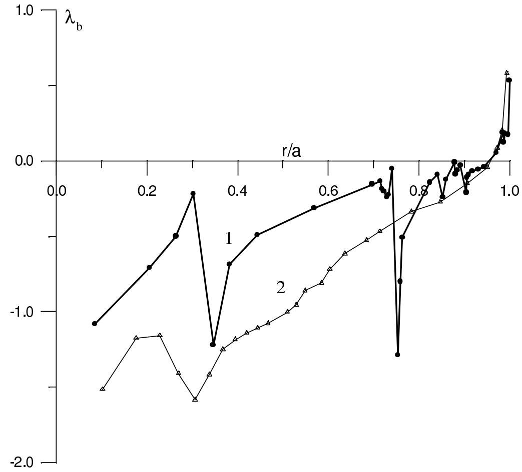

Fig. 2: Same as Figure 1 for a field produced as a result of a PIES run with $\beta = 0.01$ (curve 1).

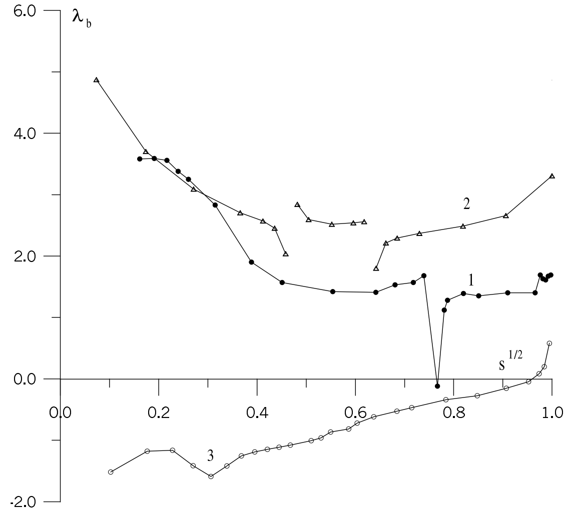

Fig. 3: Parameter λ_b for the quasi-helical equilibrium [2] at $< \beta >$=0.058 (curve 1) and at β=0 (curve 2); curve 3 shows λ_b for the W7-X Boozer data corresponding to finite beta equilibrium with a fixed boundary (coincides with curves 2 in Figs. 1 and 2).